BJ www.biochemj.org

Biochem. J. (2010) **432**, 595–605 (Printed in Great Britain) doi:10.1042/BJ20101032

BJ Cell

online data

595

Lack of DNA helicase Pif1 disrupts zinc and iron homoeostasis in yeast

María GUIROLA*[1], Lina BARRETO†[1], Ayelen PAGANI*, Miriam ROMAGOSA*, Antonio CASAMAYOR†, Silvia ATRIAN*[2] and Joaquín ARIÑO†[2,3]

*Departament de Genètica and Institut de Biomedicina, Universitat de Barcelona, Barcelona, Spain, and †Departament de Bioquímica i Biologia Molecular and Institut de Biotecnologia i Biomedicina, Universitat Autònoma de Barcelona, Bellaterra 08193, Barcelona, Spain

The *Saccharomyces cerevisiae* gene *PIF1* encodes a conserved eukaryotic DNA helicase required for both mitochondrial and nuclear DNA integrity. Our previous work revealed that a *pif1*Δ strain is tolerant to zinc overload. In the present study we demonstrate that this effect is independent of the Pif1 helicase activity and is only observed when the protein is absent from the mitochondria. *pif1*Δ cells accumulate abnormal amounts of mitochondrial zinc and iron. Transcriptional profiling reveals that *pif1*Δ cells under standard growth conditions overexpress aconitase-related genes. When exposed to zinc, *pif1*Δ cells show lower induction of genes encoding iron (siderophores) transporters and higher expression of genes related to oxidative stress responses than wild-type cells. Coincidently, *pif1*Δ mutants are less prone to zinc-induced oxidative stress and display a higher reduced/oxidized glutathione ratio. Strikingly, although *pif1*Δ cells contain normal amounts of the Aco1 (yeast aconitase) protein, they completely lack aconitase activity. Loss of Aco1 activity is also observed when the cell expresses a non-mitochondrially targeted form of Pif1. We postulate that lack of Pif1 forces aconitase to play its DNA protective role as a nucleoid protein and that this triggers a domino effect on iron homoeostasis resulting in increased zinc tolerance.

Key words: aconitase, iron homoeostasis, Pif1, *Saccharomyces cerevisiae*, zinc homoeostasis.

INTRODUCTION

Zinc is an essential metal for all organisms, participating in the structure and/or function of many proteins. Although redox inactive, zinc excess is deleterious to cells. The budding yeast *Saccharomyces cerevisiae* is not an exception and homoeostatic mechanisms exist that ensure cellular responses to both zinc deficiency and surplus. The cellular response to zinc deficiency has been thoroughly characterized (for a review, see [1]). The vacuole has been identified as the storage system for zinc [2–4], but beyond that little is known about the cellular mechanisms that are induced by or regulate zinc excess [5].

Previously, our group reported a genome-wide study of the molecular effects caused by high zinc levels in *S. cerevisiae*, by combining a screen of the haploid deletion library with transcriptomic profiling [6]. We confirmed the requirement of numerous chaperones for proper protein folding or targeting to the vacuole and mitochondria. Additionally, several genes involved in the stress response (mainly oxidative), sulfur metabolism, as well as components of the iron regulon were identified as crucial components of cellular resistance to high zinc. We also showed that exposure to high zinc generates ROS (reactive oxygen species), which paradoxically is exactly the same effect produced by zinc starvation [7]. Significantly, zinc excess results in a concomitant decrease of intracellular iron levels, as well as Aco1 (yeast aconitase) and cytochrome *c* activities in stationary-phase cultures. These results suggest that high zinc may alter the assembly and/or function of iron-sulfur-containing proteins, thus establishing a link between zinc, iron and sulfur metabolism.

Our screen highlighted a unique deletion mutant exhibiting a clear high-zinc-tolerance phenotype. In zinc-supplemented medium, cells lacking the *PIF1* gene grew much better than wild-type cells. Pif1 is a DNA helicase, conserved from yeast to humans [8] (for a review, see [9]). In yeast, Pif1 has been associated with the maintenance of mtDNA (mitochondrial DNA) [10], as *pif1*Δ mutants tend to lose their mtDNA due to their incapacity to efficiently perform mtDNA repair and recombination [11,12]. These deficiencies lead to a temperature-dependent *petite* phenotype [13]. A nuclear role, as an inhibitor of telomere elongation via displacing telomerase from its substrate [14,15], has also been proposed for Pif1 [16].

The role of Pif1 in DNA maintenance provided no clues to explain the increase in zinc tolerance observed for the *pif1*Δ mutation. However, the fact that aconitase has been shown to be essential for mtDNA maintenance independent of its catalytic activity [17], together with a report showing that overexpression of *ACO1* suppressed the mtDNA instability in the *pif1*Δ mutant [18], suggests a functional link between both proteins. Because of the relevant role of aconitase in metal homoeostasis, we decided to re-examine the effect of *pif1*Δ on the cellular response to zinc overload, thus expanding on our knowledge of zinc homoeostasis in wild-type cells [6]. We found that zinc and iron homoeostasis is altered in *pif1*Δ mutants and that these cells completely lack aconitase activity. It is known that Aco1 is an iron-sulfur-cluster-containing enzyme that acts as a sensor of cellular iron status [19]. This fact, together with the strong epistasis of *ACO1* with *PIF1* leads us to postulate that lack of Pif1 may force Aco1 to strengthen its mtDNA protective role as a nucleoid protein, with loss of its enzymatic activity, which would trigger a domino effect on iron homoeostasis resulting in increased zinc tolerance. Therefore the multifunctional nature of yeast aconitase [20,21] would be at the crossroad of the pleiotropic effect of *PIF1* deletion.

Abbreviations used: BPS, bathophenantroline disulfonic acid; mtDNA, mitochondrial DNA; ORF, open reading frame; ROS, reactive oxygen species.

[1] These authors contributed equally to this work.

[2] These authors contributed equally as co-last authors.

[3] To whom correspondence should be addressed (email joaquin.arino@uab.es).

EXPERIMENTAL

Yeast strains and culture conditions

Yeast strains used in the present study are described in Table 1. Growth tests on agar plates (dot tests) were carried out by spotting 3 μl of culture dilutions (starting at a D_{600} of 0.05) and incubating at 28 °C for the indicated times. Growth tests in liquid cultures were carried out as follows: overnight cultures were diluted in 310 μl of YPD medium [1 % (w/v) yeast extract/2 % (w/v) peptone/2 % (w/v) glucose] up to a D_{600} of 0.01 in 96-well plates with or without the appropriate additions (i.e. $ZnCl_2$) and growth resumed at 28 °C for 24–48 h. The D_{595} nm was determined in a Thermo Multiskan Ascent 96-well reader.

Cell culture conditions for metal accumulation measurements

S. cerevisiae strain BY4741 and its derivative mutant *pif1*Δ were grown in YPD medium until the exponential phase (D_{600} of 0.6). Growth was resumed in the absence or the presence of 5 mM $ZnCl_2$ for 24 h, when the stationary phase (D_{600} of $\sim$2.5–3.0, depending on the zinc concentration) was reached. Samples containing 40 and 80 D_{600} of cells (for total metal content and mitochondrial metal content respectively) were taken at the moment of metal addition and after 24 h.

Total and mitochondrial metal content measurement

Cellular metal content was measured by inductively coupled plasma-atomic emission MS in a Polyscan 61E apparatus (Thermo Jarrell Ash), as described in [6]. Mitochondria were isolated using a yeast mitochondria isolation kit (MITOISO3, Sigma–Aldrich). The quality of the isolation process was evaluated by Western blotting using an rabbit polyclonal antiserum (1:8000 dilution) developed against cytochrome *c* (Cyt1, a gift from D. Pain; Department of Pharmacology and Physiology, UMDNJ, New Jersey Medical School, Newark, NJ, U.S.A.) and anti-vacuolar carboxypeptidase Y antibody [dilution: 1:7500, a gift from M. Geli; Institut de Biologia Molecular de Barcelona (IBMB-CSIC), Barcelona, Spain]. This analysis indicated that mitochondrial preparations were devoid of vacuolar contamination (Supplementary Figure S1 at http://www.BiochemJ.org/bj/432/bj4320595add.htm). Metal measurements were made as described for cellular content, except that inductively coupled plasma-MS was used for determinations using an Eland-6000 apparatus (PerkinElmer).

RNA purification, cDNA synthesis and DNA microarray experiments

For RNA purification, 25 ml of yeast cultures were grown at 28 °C in YPD medium until they reached a D_{660} of 0.6. Yeast cells were cultured for an additional 1 h, in the presence or absence of 5 mM $ZnCl_2$. Cells were harvested by centrifugation (1200 ***g*** for 5 min) and washed with cold water. Dried cell pellets were kept at -80 °C until RNA purification. Total RNA was purified using the RiboPure yeast kit (Ambion) following the manufacturer's instructions. RNA quality was assessed by electrophoresis in a denaturing 0.8 % agarose gel and quantified by measuring A_{260} in a BioPhotometer (Eppendorf).

Transcriptional analyses were performed using DNA microarrays containing PCR-amplified fragments from 6014 *S. cerevisiae* ORFs (open reading frames) [22,23] as described previously [6]. For each experimental condition a dye-swapping experiment was performed. The fluorescent intensity of the spots was measured and processed using the GenePix Pro 6.0 software (Molecular Devices). Spots with either a diameter smaller than 120 μm, or fluorescence intensity for Cy3 (indocarbocyanine) and Cy5 (indodicarbocyanine) lower than 150 units, were not considered for further analysis. A given gene was considered to be induced or repressed when the ratio between the two compared samples was higher than 1.8 or lower than 0.55 respectively. Genes whose expression was considered changed in any of the tested mutants were selected for further analyses. The GEPAS server (http://gepas.bioinfo.cipf.es) was used to pre-process the data and to establish correlations between expression patterns [24]. Expression profile analysis of the selected genes was determined with EPCluster [25]. Gene ontology analysis was performed using the 'GO Term Finder' tool on the *Saccharomyces* Genome Database server (http://www.yeastgenome.org/). When wild-type and *pif1*Δ profiles were compared, the level of Pif1 dependence for expression was set as follows: genes showing a ratio $0.67 > X > 0.50$ were considered 'weakly dependent'; those with a ratio $0.50 > X > 0.25$ were ranked as 'strongly dependent' and those with a ratio < 0.25 were labelled as 'totally dependent'. Similarly, genes induced more than 2.5-fold in one strain and considered not induced (i.e. a ratio with/without zinc < 1.3) in the other strain were also considered as totally dependent. Microarray data can be retrieved from the Gene Expression Omnibus (http://www.ncbi.nlm.nih.gov/geo/) under record number GSE18411. Genes encoding mitochondrial proteins were extracted with the gene ontology 'slim mapper' tool at the *Saccharomyces* Genome Database [26].

Evaluation of ROS formation and measurement of glutathione levels

Evaluation of ROS formation was carried out as in [6] using wild-type BY4741 cells and its isogenic derivative *pif1::kanMX*. $ZnCl_2$ was added to a final concentration of 10 mM. Parallel cultures received 5 mM H_2O_2. Fluorescence in each sample was calculated using Wasabi software. Approx. 600 cells per condition were selected from diverse Nomarski images and the intensity of its fluorescence automatically measured from the fluorescence image. Background values were obtained from several areas devoid of cells and subtracted. The average fluorescence per condition was then calculated. Glutathione levels were measured as described previously [6].

Measurement of aconitase activity and protein content

Strains were grown as described for metal determination except that 20 and 25 absorbance units were collected for protein quantification and activity assay samples respectively, and that cells were taken at stationary phase (24 h). A BY4741 *aco1*Δ derivative mutant (lacking the yeast mitochondrial aconitase gene) was grown under the same conditions and was used as the control in the aconitase protein and activity assays.

Aconitase activity was determined essentially as in [6]. The aconitase contents were measured in total cell extracts and also in mitochondrial and non-mitochondrial fractions. Total cell extract was prepared from 20 absorbance units of cells, which were harvested (1200 ***g*** for 5 min), washed, and resuspended in 0.1 ml of 100 mM Tris/HCl, pH 8.0, plus 1 mM PMSF and proteases inhibitors (Complete™ EDTA-free; Roche). Cells were broken with the aid of glass beads. After a 15-min spin at 15700 ***g***, in a microfuge, the supernatant was separated and stored at -20 °C. Total protein content was determined by using the Quick Start™ Bradford protein assay kit (Bio-Rad) with BSA as the standard.

Table 1 Yeast strains used in the present study

Strain	Genotype	Source/reference
BY4741	*MATa his3*Δ1 *leu2*Δ0 *met15*Δ0 *ura3*Δ0	Euroscarf
BY4741 *pif1*	BY4741 *pif1::kanMX*	Euroscarf
BY4741 *aco1*	BY4741 *aco1::kanMX*	Euroscarf
BY4741 *fet3*	BY4741 *fet3::kanMX*	Euroscarf
BY4741 *fit3*	BY4741 *fit3::kanMX*	Euroscarf
BY4741 *ftr1*	BY4741 *ftr1::kanMX*	Euroscarf
W303-1A	*MATa ade2 can1 his3 leu2 trp1 ura3*	R. Rothstein
LBY65	W303-1A *pif1::kanMX*	Present study
DBY746	*MAT*α *his3-1 leu2-3,112 ura3-52 trp1-289*	D. Botstein
LBY67	DBY746 *pif1::kanMX*	Present study
YPH499	*Mata ura3-52 lys2-801 ade2-101 trp1-*Δ*63 his3-*Δ*200 leu2-*Δ*1*	[44]
YPH499 *pif1*	YPH499 *pif1::TRP1*	[16]
pif1-K264A	YPH499 *pif1*-K264A	[14]
YPH499 *pif1-m1*	YPH499 *pif1-m1*	[14]
YPH499 *pif1-m2*	YPH499 *pif1-m2*	[14]

Mitochondrial and non-mitochondrial fractions were collected following the yeast mitochondria isolation kit protocol (MITOISO3). The aconitase content was measured by a quantitative ELISA. Plates (IWAKI, Japan) were coated with 30 μg/ml cell extract or a standard curve starting on 4 μg/ml of aconitase (from porcine heart; Sigma–Aldrich) in carbonate buffer. Serial dilutions were made and the final volume was kept in 100 μl. The coating step was performed overnight at 4 °C. After the plates were washed with PBS containing 0.5 % Tween 20, a blocking solution of PBS containing 1 % (w/v) BSA and 0.5 % Tween 20 was added for 1 h at 37 °C. A rabbit polyclonal antisera against Aco1 (a gift from A. Dancis; Division of Hematology/Oncology, University of Pennsylvania, Philadelphia, PA, U.S.A.) was added to a final dilution of 1:10000 and then incubated overnight at 4 °C. After three washes, the plates were incubated with anti-(rabbit IgG)–horseradish peroxidase (Amersham Biosciences) at 37 °C for 1 h. Finally, plates were washed once more and the substrate, 3 % H_2O_2 and 0.5 mg/ml *o*-phenylenediamine in 0.1 M citrate buffer, pH 5, was used to develop the chromogenic reaction that was chemically stopped after 15 min. The A_{492} was determined in a plate reader. The aconitase concentration from the samples was calculated using the standard curve as a reference.

RESULTS

Characterization of tolerance to zinc in *pif1*Δ mutants

The isolation in our previous screen of a *pif1* deletion mutant as a prominent zinc-hypertolerant strain prompted us to characterize the basis of this phenotype. Increased tolerance to zinc can be observed when *PIF1* is deleted in different genetic backgrounds, such as BY4741 and YPH499 (Figure 1A) or DBY746 and W303-1A (results not shown). It has been established that Pif1 displays helicase activity, which is involved in mtDNA repair and telomere length regulation. Expression of an allele carrying the K264A mutation, which generates a protein unable to effectively bind ATP and thus lacking helicase activity [14], yielded cells with a wild-type tolerance to zinc (Figure 1A). This observation indicates that the loss of Pif1 helicase activity was not the cause for the increased zinc tolerance of the *pif1*Δ mutant. We then determined whether the effect of Pif1 on zinc tolerance was related to its nuclear or mitochondrial localization. Two different alleles of *PIF1* were expressed: *pif1-m1*, which encodes a protein targeted to the nucleus, and *pif1-m2*, which produces a protein largely found in the mitochondria [16]. Expression of the nuclear-targeted version resulted in cells with zinc tolerance equivalent to that of the *pif1*Δ strain, indicating that this version does not act as a wild-type Pif1 on zinc tolerance (Figure 1B). In contrast, expression

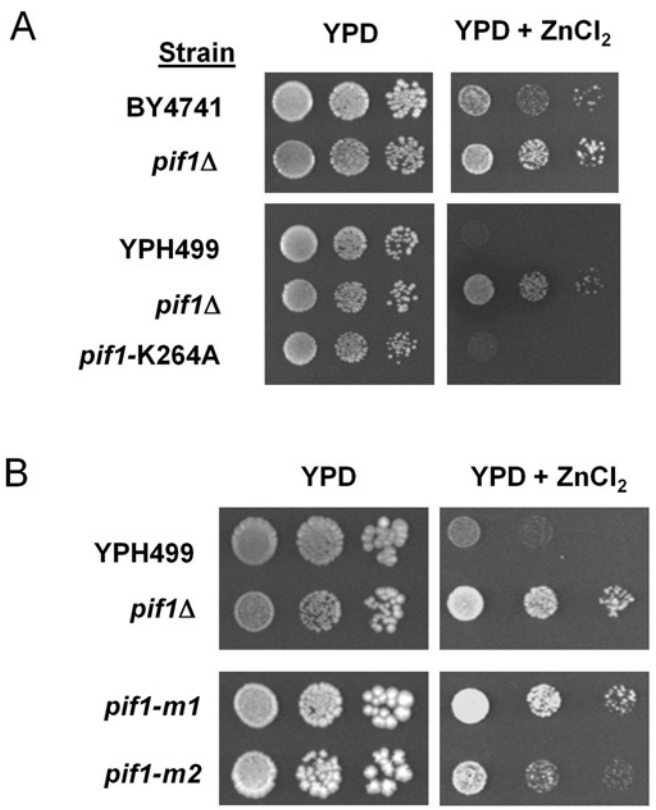

Figure 1 Lack of Pif1 confers tolerance to zinc

(**A**) Wild-type strains BY4741 (upper panels) and YPH499 (lower panels) and their *pif1* derivatives were spotted on to YPD plates in the absence or presence of 5 or 7 mM $ZnCl_2$ respectively. A strain carrying a *pif1* allele devoid of helicase activity (*pif1*-K264A) is included. Plates were incubated for 3 (BY4741 background) or 4 (YPH499 background) days. (**B**) YPH499-derived strains carrying a deletion of *PIF1* (*pif1*Δ) or expressing version of the protein targeted to the nucleus (*pif1-m1*) or to the mitochondria (*pif1-m2*) were spotted on YPD plates in the absence or presence of 5 mM $ZnCl_2$ and grown for 4 days.

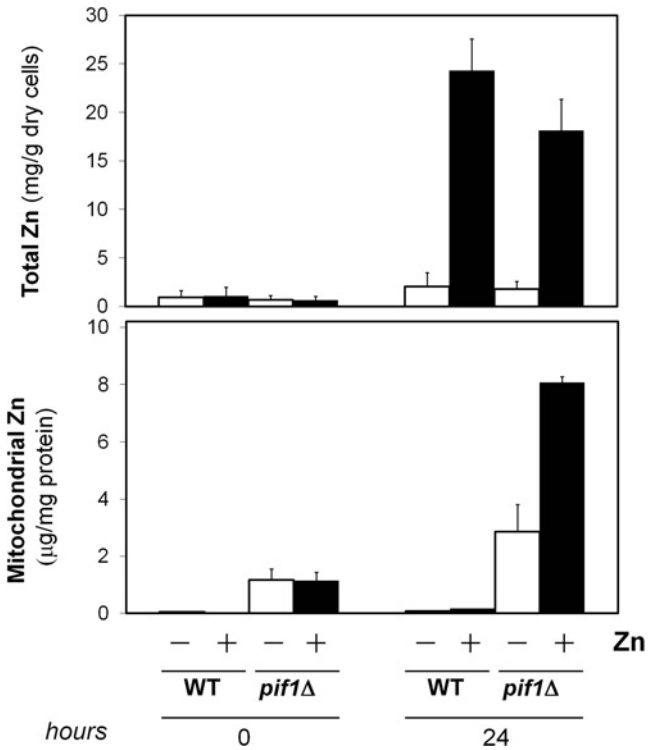

Figure 2 Effect of the *pif1*Δ mutation on total and mitochondrial zinc content

Wild-type (WT) BY4741 and its *pif1*Δ derivative were grown as described in the Experimental section. Cells were collected from untreated (−) or 5 mM $ZnCl_2$-treated (+) cultures at the moment of zinc addition (0 h) or after 24 h. Total zinc (upper panel) or mitochondrial zinc (lower panel) contents were measured. Results are means ± S.D. for six independent experiments.

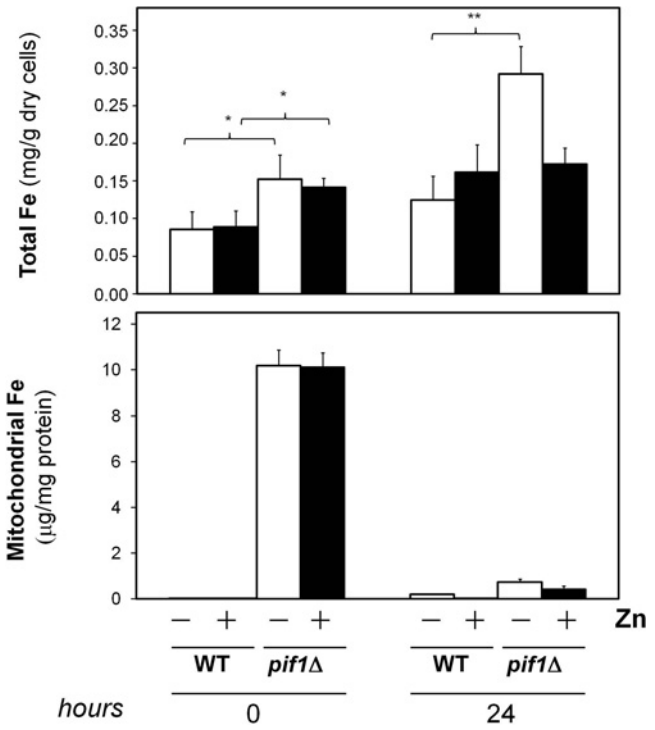

Figure 3 Effect of the *pif1*Δ mutation on total and mitochondrial iron content

Cells were cultured as described in the legend of Figure 2 and total iron (upper panel) or mitochondrial iron (lower panel) contents were measured. Results are means ± S.D. for six independent experiments. $^*P < 0.05$; $^{**}P < 0.01$ (as assessed with the Newman–Keuls multiple comparison test). WT, wild-type.

of *pif1-m2* yielded cells clearly less tolerant to zinc than the deletion mutant. These experiments demonstrate that it is the loss of mitochondrially localized Pif1 protein which leads to zinc hypertolerance.

Effect of the *pif1* mutation on total and mitochondrial zinc and iron contents

In our previous report [6] we demonstrated that high zinc levels disrupted iron homoeostasis. Therefore we investigated the levels of both metals in wild-type and *pif1*Δ cells growing in normal and zinc-supplemented medium. Given the importance of the mitochondrial localization of Pif1 for normal zinc tolerance (Figure 1B), the level of these metals was also measured in mitochondrial extracts. Exponential cultures were grown for 24 h in the absence or the presence of 5 mM zinc. At the end of the incubation in the absence of added zinc, the cellular zinc content was the same for wild-type and *pif1* cells. In contrast, mitochondrial zinc was significantly higher in the mutant (2.86 ± 0.39 μg/mg of protein) than in the wild-type strain (0.072 ± 0.023 μg/mg of protein) (Figure 2). The differences between the wild-type and *pif1*Δ cells were even more dramatic when these cells were grown in zinc-supplemented medium. Total zinc content increased in both wild-type and *pif1* strains, although the amount was slightly lower in the mutant strain. However, mitochondrial zinc content was dramatically increased in *pif1* cells, reaching values of 8.06 ± 0.21 μg/mg of protein (Figure 2). These values represent an increase of 5.7-fold when mitochondrial/total zinc ratio is calculated. All of these results highlight an unreported phenotype of mitochondrial zinc hyperaccumulation for *pif1*Δ cells.

Analysis of total and mitochondrial iron levels in the exponentially growing cultures revealed that the lack of Pif1 resulted in higher total cellular iron content (Figure 3). Whereas mitochondrial iron in wild-type cells was very low (0.023 ± 0.007 μg/mg of protein), it spectacularly increased in *pif1*Δ mutants (10.18 ± 0.68 μg/mg of protein). After 24 h of growth in the absence of added zinc, the total iron content of *pif1*Δ cells increased. However, this increase was not observed in zinc-supplemented cells. It is worth noting that regardless of the addition of zinc to the medium, the large increase in mitochondrial iron observed in the exponentially growing *pif1*Δ mutant was not observed in stationary cells.

These results are consistent with the notion that the tolerance to zinc of the *pif1*Δ mutant is based on a higher cellular iron content. Accordingly, we observed that lack of the reductive high-affinity iron transport system, encoded by the *FTR1* and *FET3* genes, results in a slight but perceptible decrease in zinc tolerance (Figure 4A), a phenotype that was unnoticed in our previous genome-wide screen [6]. In contrast, as expected, deletion of the siderophore transporter-encoding gene *FIT3* has no effect, given that yeast does not synthesize siderophores. Interestingly, chelating iron in the medium by addition of BPS (bathophenantroline disulfonic acid) significantly reduced tolerance to zinc, not only in the wild-type strain, but also the protective effect of the *pif1*Δ mutation in front of an excess of zinc. In contrast, supplementation of the medium with iron in the micromolar range further increased the tolerance to zinc of both wild-type cells and the *pif1*Δ mutant, although for the latter

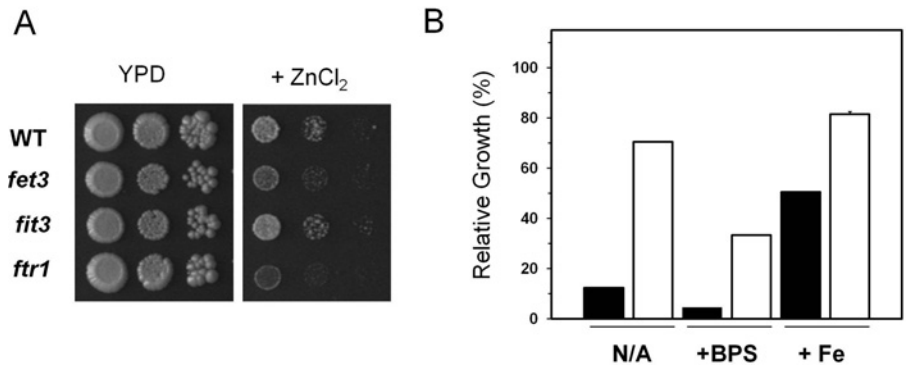

Figure 4 Effect of iron availability on zinc tolerance of wild-type and *pif1*Δ cells

(**A**) Wild-type strain BY4741 and the indicated *kanMX*-deletion derivatives were spotted on to YPD plates with or without 5 mM $ZnCl_2$. Growth was monitored after 4 days. (**B**) Wild-type strain BY4741 (black bars) and the *pif1*Δ mutant (white bars) were inoculated at a D_{600} of 0.01 on liquid YPD medium containing 4 mM $ZnCl_2$, with no further addition (N/A), 75 μM BPS (+BPS) or 100 μM $Fe(NH_4)_2(SO_4)_2$ (+Fe). Growth was monitored at 595 nm after 48 h. For each strain, results correspond to growth relative to that of the culture without added zinc and are the means ± S.E.M. for three cultures.

the effect was rather small (Figure 4B). This suggests that the observed effects are not caused by a competitive entry of zinc and iron through the low-affinity Fet4 transporter. Overall, our results indicate that a patent deregulation of mitochondrial zinc and iron content results from deletion of *PIF1* and suggest that iron availability could be a key factor for zinc tolerance not only for wild-type cells, but also constitute the basis for the observed *pif1*Δ tolerant phenotype.

Transcriptomic profiles of the *pif1* mutant

Comparison of the transcriptomic profile of wild-type and *pif1*Δ cells exponentially growing in YPD medium revealed a relatively small number of changes. A total of 56 genes appeared induced at least 1.8-fold in the *pif1*Δ mutant (Table 2). Gene ontology analysis revealed that the induced genes included several tricarboxylic acid cycle-related genes (*ACO1*, *ACO2*, *IDH1* and *IDH2*). In addition, other genes such as *LYS4* and *LEU1*, encoding aconitase-like sulfur-iron-cluster proteins, were also induced. Expression of diverse genes responsive to hypoxia or involved in adaptation to this condition, and of three genes encoding helicase-related activities (*DSS1*, *DHH1* and *YHR218W*) was also increased. Interestingly, we observed an excess of genes related to mitochondrial functions (15 genes, accounting for 27 % of induced genes compared with the expected 16.5 %, see Table 2). Only 24 genes were found to be less expressed in *pif1*Δ than in wild-type cells, among them four related to the metabolism of cysteine and methionine (*STR3*, *MET16*, *MUP3* and *MET1*).

Since mutation of *PIF1* results in increased tolerance to zinc, we considered it necessary to evaluate how the absence of Pif1 would affect the transcriptional changes derived from exposure to this metal. To this end, we compared these datasets (Figure 5). We observed that exposure of wild-type cells to 5 mM zinc for 60 min resulted in increased expression of 270 genes, whereas in *pif1*Δ cells we detected 244 genes (Figure 5). Among the 240 genes induced in the wild-type and with valid data for the *pif1*Δ strain, 81 were less expressed in *pif1*Δ cells. Four genes were considered totally dependent of the presence of Pif1, 19 were rated as strongly dependent and 58 were defined as weakly dependent (see the Experimental section for the definitions). Gene ontology analysis of genes induced by zinc in a Pif1-dependent fashion, revealed an excess of siderophore-utilization-encoding genes (i.e. *FIT1*, *ARN1*, *ARN2*, *FIT2* and *FIT3*; *P*-value of 5.6×10^{-6}; see Figure 5, cluster 1). In contrast, 26 genes were more induced in *pif1*Δ cells exposed to zinc than in wild-type cells under the same conditions (one totally dependent, four strongly dependent and 21 weakly dependent). Among them, an excess (*P*-value of 2.9×10^{-5}) of genes induced in response to oxidative stress, such as *GPX2*, *CTT1*, *TRX2*, *SOD1*, *AHP1* and *TSA1*, were identified (Figure 5, cluster 2).

Therefore our results suggest that lack of *Pif1* in cells subjected to zinc-overload leads to increased expression of oxidative-stress-response genes and decreased expression of genes encoding iron (mostly siderophores) transporters. We then evaluated the tolerance to 5 mM zinc of 26 deletion mutants for genes classified as functionally related to oxidative stress response [FunCat (Functional Catalogue) 32.01.01]. As shown in Supplementary Figure S2 (at http://www.BiochemJ.org/bj/432/bj4320595add.htm), only four mutants displayed altered sensitivity to zinc. Two of them, *tsa1* and *sod1* were very sensitive, whereas deletion of *PRX1* and *SOD2* yielded cells slightly tolerant to the metal. Neither these two mutant strains, nor the *izh3* or *izh4* mutants, previously reported as zinc-tolerant [27], were identified in our previous screen [6], probably because of their relatively slight phenotype.

*pif1*Δ cells are protected against zinc-induced oxidative stress

Previous work showed that an excess of zinc in the medium resulted in oxidative stress [6]. As shown above, genes responsive to oxidative stress are more induced in *pif1*Δ cells exposed to zinc than in wild-type cells. We investigated the effect of the *pif1*Δ mutation in zinc-induced ROS formation by means of fluorescent dihydrorhodamine 123 staining. As shown in Figures 6(A) and 6(B), fluorescence induced by treatment with 10 mM $ZnCl_2$ was attenuated in the *pif1*Δ mutant, indicating a lower level of ROS. This effect was specific for zinc treatment, since ROS generation caused by exposure to 5 mM H_2O_2 was not decreased in *pif1*Δ cells. The notion that the effect of the *pif1*Δ mutation is zinc-specific is reinforced by the observation that, whereas they are tolerant to zinc, *pif1*Δ cells are more sensitive than wild-type cells to diverse oxidative agents, such as H_2O_2, menadione or diamide (Figure 6C).

Exposure to zinc is known to increase the oxidized/total glutathione ratio. As shown in Figure 7, *pif1*Δ cells display

Table 2 Genes differentially induced (>1.8-fold) in a *pif1*Δ mutant

The asterisk indicates gene products with recognized mitochondrial functions. TCA, tricarboxylic acid.

ORF	Gene	Induction (-fold)	Mit.	Features
TCA cycle and aconitase-like				
YOR135C	*IRC14*	3.45		Partially overlaps *IDH1*
YLR304C	*ACO1*	3.13	(*)	Aconitase, required for the TCA cycle and for mitochondrial genome maintenance
YGL009C	*LEU1*	2.96		Isopropylmalate isomerase (leucine biosynthesis pathway)
YOR136W	*IDH2*	2.67	(*)	Subunit of mitochondrial NAD^+-dependent isocitrate dehydrogenase
YDR234W	*LYS4*	2.50	(*)	Homoaconitase, catalyses the conversion of homocitrate into homoisocitrate (lysine biosynthesis pathway)
YNL037C	*IDH1*	2.37	(*)	Subunit of mitochondrial NAD^+-dependent isocitrate dehydrogenase
YJL200C	*ACO2*	1.84	(*)	Putative mitochondrial aconitase isozyme
Hypoxia/anaerobic/respiratory				
YGL162W	*SUT1*	3.22		Transcription factor involved in induction of hypoxic gene expression
YIL011W	*TIR3*	2.63		Cell-wall mannoprotein expressed under anaerobic conditions
YKR066C	*CCP1*	2.00	(*)	Mitochondrial cytochrome *c* peroxidase, degrades reactive oxygen species in mitochondria
YKL109W	*HAP4*	1.91		Major subunit of the Hap2p/3p/4p/5p CCAAT-binding complex
YER011W	*TIR1*	1.85		Cell-wall mannoprotein induced by anaerobiosis
Helicase activity				
YMR287C	*DSS1*	2.57	(*)	3'→5' Exoribonuclease, associated with the ATP-dependent RNA helicase Suv3p
YDL160C	*DHH1*	2.32		Cytoplasmic DExD/H-box helicase, stimulates mRNA decapping
YHR218W	*YHR218W*	1.81		Helicase-like protein encoded within the telomeric Y′ element
Other				
YKR093W	*PTR2*	3.22		Integral membrane peptide transporter, mediates transport of di- and tri-peptides
YLL013C	*PUF3*	2.90	(*)	Protein of the mitochondrial outer surface
YDL037C	*BSC1*	2.79		Protein of unconfirmed function
YMR153W	*NUP53*	2.73		Subunit of the nuclear pore complex
YMR068W	*AVO2*	2.72		Component of a complex containing the Tor2p kinase and other proteins
YCL020W	*YCL020W*	2.67		Retrotransposon TYA Gag gene co-transcribed with TYB Pol
YBR040W	*FIG1*	2.62		Integral membrane protein required for efficient mating
YMR211W	*DML1*	2.55	(*)	Essential protein involved in mtDNA inheritance
YNL202W	*SPS19*	2.41		Peroxisomal 2,4-dienoyl-CoA reductase
YOL041C	*NOP12*	2.28		Nucleolar protein involved in pre-25S rRNA processing and biogenesis of large 60S ribosomal subunit
YKL161C	*YKL161C*	2.25		Protein kinase implicated in the Slt2p signalling pathway
YHR036W	*BRL1*	2.18		Essential nuclear envelope integral membrane protein
YNL023C	*FAP1*	2.14		Protein that binds to Fpr1p, conferring rapamycin resistance
YHR072W	*ERG7*	2.09		Lanosterol synthase, an essential enzyme in ergosterol biosynthesis
YPL144W	*POC4*	2.08		Component of a heterodimeric Poc4p–Irc25p chaperone involved in assembly of α subunits into the 20S proteasome
YFL-TyA	*YFL-TyA*	2.05		
YGL194C	*HOS2*	2.03		Histone deacetylase
YLR382C	*NAM2*	2.00	(*)	Mitochondrial leucyl-tRNA synthetase
YDL231C	*BRE4*	1.95		Zinc-finger protein containing five transmembrane domains
YDR345C	*HXT3*	1.93		Low-affinity glucose transporter of the major facilitator superfamily
YBL103C	*RTG3*	1.90		Basic helix-loop-helix-leucine zipper transcription involved in the retrograde and TOR pathways
YBR238C	*YBR238C*	1.89	(*)	Mitochondrial membrane protein
YOR178C	*GAC1*	1.83		Regulatory subunit for Glc7p type-1 protein phosphatase
YIL009W	*FAA3*	1.83		Long-chain fatty acyl-CoA synthetase
YDL021W	*GPM2*	1.83		Homologue of Gpm1p phosphoglycerate mutase
YJL187C	*SWE1*	1.83		Protein kinase that regulates the G_2/M transition by inhibition of Cdc28p kinase activity
YOL105C	*WSC3*	1.83		Partially redundant sensor-transducer of the stress-activated PKC1/MPK1 pathway
YBR177C	*EHT1*	1.82	(*)	Acyl-coenzymeA:ethanol O-acyltransferase
YAR042W	*SWH1*	1.81		Protein similar to mammalian oxysterol-binding protein
YBR001C	*NTH2*	1.81	(*)	Putative neutral trehalase
YNL197C	*WHI3*	1.80		RNA-binding protein that sequesters CLN3 mRNA in cytoplasmic foci
Uncharacterized				
YKL071W	*YKL071W*	2.86		Putative protein of unknown function
YHL049C	*YHL049C*	2.52		Putative protein of unknown function
YER076C	*YER076C*	2.21	(*)	Putative protein of unknown function
YBR113W	*YBR113W*	2.20		Dubious open reading frame, partially overlaps the verified gene CYC8
YGL088W	*YGL088W*	2.07		Dubious open reading frame, partially overlaps snR10
YGL239C	*YGL239C*	2.06		Dubious open reading frame, partially overlaps verified gene CSE1
YBL012C	*YBL012C*	1.88		Dubious open reading frame
YJL078C	*PRY3*	1.88		Protein of unknown function
YFL032W	*YFL032W*	1.86		Dubious open reading frame, partially overlaps the verified gene HAC1/YFL031W

lower total glutathione content both under normal or zinc-stressed conditions. Under normal growth conditions, the amount of oxidized glutathione was approx. 4-fold lower in *pif1*Δ cells than in the wild-type strain. Exposure to 6 mM zinc strongly increased the amount of oxidized glutathione in wild-type cells but had a lesser effect in the *pif1*Δ strain. Consequently, in these conditions the reduced/oxidized glutathione ratio was approx. 4-fold higher in *pif1*Δ mutants than in wild-type cells (Figure 7, bottom panel). This is consistent with the less-intense zinc-induced oxidative stress observed in *pif1*Δ cells.

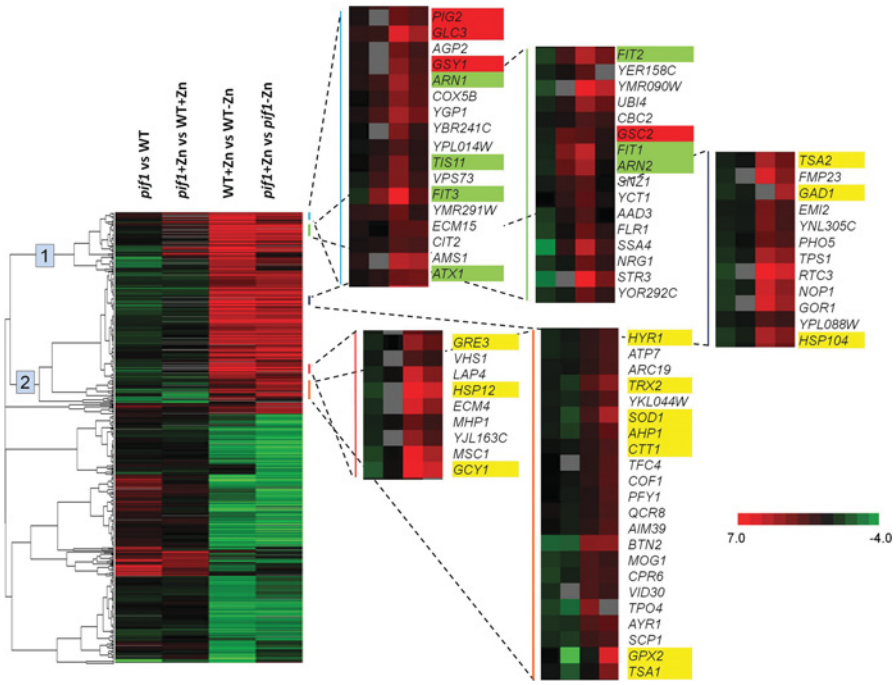

Figure 5 Gene expression changes induced by lack of *PIF1* in the absence or the presence of excess zinc

Cluster analysis of the expression profiles acquired. The selected datasets (*pif1*Δ mutant compared with wild-type cells growing on YPD or YPD plus 5 mM zinc for 60 min, and wild-type or *pif1*Δ cells in the absence of added zinc compared with those growing for 60 min in YPD plus 5 mM zinc) were hierarchically clustered (complete linkage clustering, uncentred correlation) by means of the Cluster (version 3.0) software and visualized with TreeView (version 1.60) [45]. Numbers refer to the selected cluster as described in the main text. Colour codes for gene function are as follows: red, glycogen metabolism; yellow, oxidative stress response; green, iron homoeostasis. WT, wild-type.

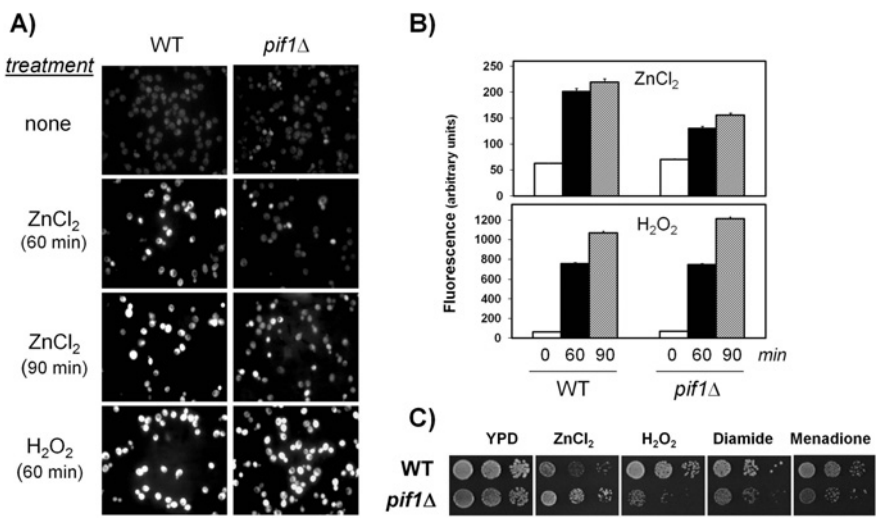

Figure 6 Effect of *pif1*Δ mutation on zinc-induced ROS formation

(**A**) Wild-type (WT) and *pif1*Δ cultures were pre-incubated with dihydrorhodamine 123 and then exposed to 10 mM $ZnCl_2$ or 5 mM H_2O_2 for 60 and 90 min (as indicated; the latter is not shown). Micrographs of representative fields are shown. The brightness of the H_2O_2-treated cells has been attenuated with respect to the rest of the micrographs, to allow proper visualization. (**B**) The intensity of fluorescence from approx. 600 cells (approx. 20 fields) was integrated as described in the Experimental section after the indicated periods of treatment. Results are expressed as means ± S.E.M. (**C**) Three dilutions of the BY4741 wild-type strain and its *pif1*Δ derivative were spotted on to YPD plates containing 5 mM $ZnCl_2$, 4 mM H_2O_2, 2.5 mM diamide or 0.125 mM menadione and incubated for 2 days (4 days for the plate containing $ZnCl_2$) until growth was recorded.

Mutation of *PIF1* dramatically affects aconitase activity

We reported previously a marked decrease in aconitase activity in wild-type cells exposed to zinc [6]. However, no aconitase activity was detected in extracts from the *pif1*Δ strain (Figure 8A) even in the absence of added zinc, with the levels similar to those of an *aco1*Δ strain, which lacks the mitochondrial aconitase gene. Aconitase activity in the *Pif1*-K264A mutant, which is devoid of helicase activity, as well as of the cells in which Pif1 was directed to the mitochondria (i.e. expressing *pif1-m2*), was

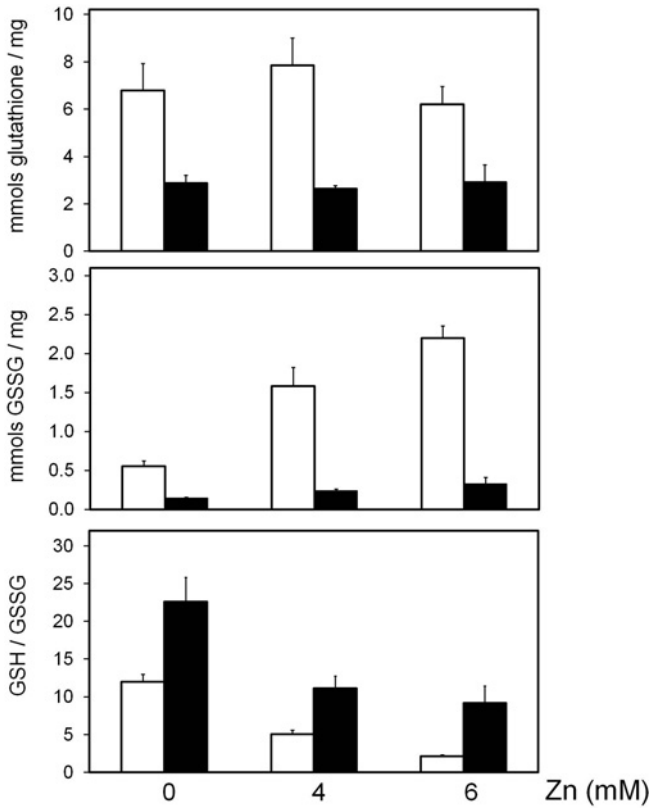

Figure 7 Glutathione content in wild-type and *pif1* cells

The wild-type BY4741 strain (white bars) and its *pif1*Δ derivative (black bars) were grown for 42 h in the absence or the presence of the indicated concentrations of $ZnCl_2$. Total (top panel) and oxidized (GSSG) (middle panel) glutathione levels were determined and are given per mg of total protein. The reduced/oxidized glutathione ratio is also represented (bottom panel). Results are means ± S.E.M. for 3–4 independent experiments.

clearly detectable, although it was somewhat lower than in wild-type cells. Conversely, those cells expressing a Pif1 exclusively targeted to the nucleus (*pif1-m1*), also lack aconitase activity (Figure 8A). Therefore the same situations that result in zinc hypertolerance also give rise to lack of aconitase activity. The effect of the absence of Pif1 on aconitase activity was confirmed in a different wild-type genetic background (BY4741; Figure 8B). Interestingly, exposure to zinc slightly increased aconitase activity in *pif1*Δ cells, although not to the wild-type strain levels in the absence of zinc (Figure 8B). In view of the absence of aconitase activity in Pif1-deficient cells, we investigated, under the same conditions, the amount of aconitase protein and its cellular distribution. Exposure of wild-type cells to zinc caused an increase in the amount of total aconitase (approx. 50 %), with essentially no alteration of the mitochondrial/non-mitochondrial distribution of the protein (Figure 8C). Remarkably, even in the absence of aconitase activity (Figures 8A and 8B) the level of the aconitase protein in untreated *pif1*Δ cells was normal and the protein was largely mitochondrial. Exposure of *pif1*Δ cells to zinc caused a moderate increase in aconitase protein, similar to that observed in the wild-type and a decrease in the relative amount of aconitase located in the mitochondria. In essence, our results indicate that the absence of aconitase activity in cells lacking Pif1 or unable to localize Pif1 to the mitochondria is not caused by the absence of aconitase protein, and that the *pif1* mutation provokes a dramatic alteration in the intracellular distribution of aconitase. It is worth noting that deletion of aconitase results in an increase in zinc tolerance comparable with that of the *pif1* mutant (Figure 8D).

DISCUSSION

Pif1 is a conserved eukaryotic helicase that in the yeast *S. cerevisiae* is involved in at least two independent processes, integrity of mtDNA [8,11] and telomere length control [16]. We report that wild-type cells exposed to zinc develop a transcriptional response that includes increased expression of several genes also induced by iron shortage. Gene activation did not affect the entire Aft1-mediated regulon, but a specific subset that is highly enriched in siderophore transporter-encoding genes. This transcription profile is reminiscent of the one observed by Crisp et al. [28,29], who demonstrated that disruption of haem biosynthesis in iron-starved cells blocks the activation of genes encoding the components of the reductive high-affinity iron transport system, but not that of siderophore-utilization-encoding genes. This observation would explain the transcription profile reported in the present study, as it has been proposed previously that an excess of zinc interferes with the biosynthesis of haem, as it competes with iron for binding to ferrochelatase [30]. Our finding that in a *pif1*Δ mutant the induction of members of the Aft1 regulon by exposure to zinc is markedly attenuated could be explained by the higher iron content of this strain, which could also explain why further addition of iron to the medium only marginally improves tolerance to zinc compared with the wild-type strain (Figure 4B).

We reported previously [6] and confirm in the present study (Figures 5 and 6) that exposure to zinc triggers a oxidative stress response that can be assessed by examination of the transcriptomic profile and the generation of ROS. In yeast, both zinc deficiency [7] and zinc overload provokes oxidative stress. It is remarkable that a similar situation has been reported for neurons [31], which suggest that yeast could be a suitable model for mitochondrial zinc homoeostasis studies. In the present study we also observe that deletion of *PIF1* decreases the generation of ROS induced by zinc (Figure 6) and results in a enhanced transcriptional response of genes encoding proteins relevant for protection against oxidative stress (e.g. *GPX2*, *CTT1*, *TRX2* and *SOD1*). Although the total amount of glutathione is lower in the *pif1*Δ mutant, the fraction of reduced glutathione is clearly higher. This difference can be observed under normal growth conditions and it is exacerbated under zinc stress. We suggest that the increased zinc tolerance of the *pif1Δ* mutant could be attributed, at least in part, to a higher capacity to deal with the oxidative stress provoked by exposure to zinc. It can be hypothesized that sequestration of zinc in the mitochondria would protect from stress. This would fit with our observation that tolerance in the *pif1*Δ mutant seems to be quite specific for zinc stress, since this strain is not tolerant to other oxidative agents, but is moderately sensitive instead.

Our results demonstrate that the absence of Pif1 protein in the mitochondria appears associated with two, apparently independent, phenotypes: the loss of aconitase activity and the hypertolerance to zinc. What could be the explanation for the absence of aconitase activity associated with the lack of Pif1 protein in the mitochondria? It has been shown previously [17] that Aco1 binds to the nucleoid structure formed by yeast mtDNA, in order to compensate for the lack of other mtDNA proteins [32,33]. It must be noted that there has been a previous study which shows that Aco1 is epistatic to Pif1 for mtDNA maintenance, due to the ability of Aco1 to bind to mtDNA through regions of the protein completely independent to those responsible for its catalytic activity [18]. We therefore hypothesize

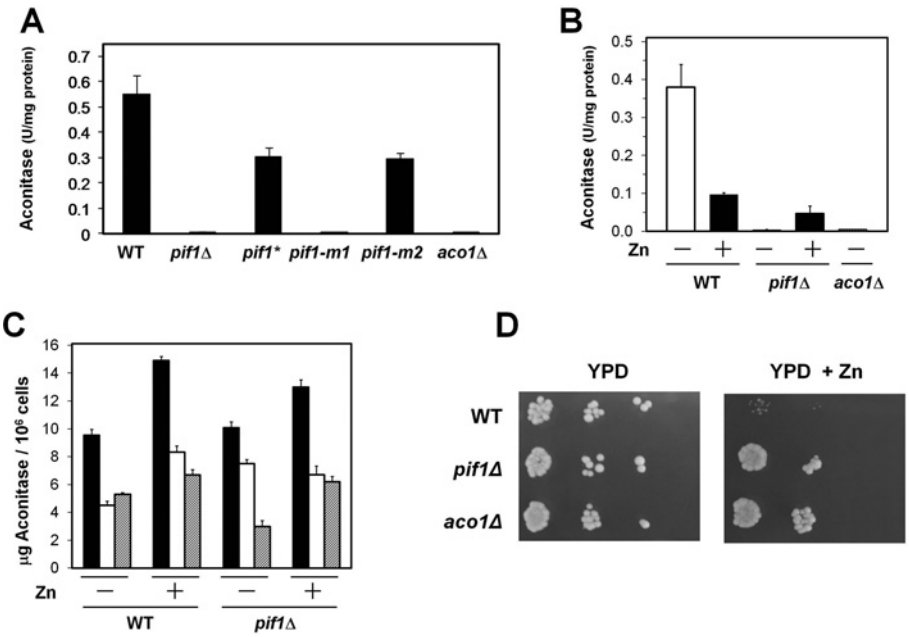

Figure 8 Functional link between Pif1, Aco1 and zinc tolerance

(**A**) Wild-type (WT) YPH499 cells and its isogenic derivatives *pif1*Δ, *pif1*-K264A (*pif1**), *pif1-m1* and *pif1-m2* were grown to the stationary phase, and aconitase activity was measured. Aconitase activity in a strain lacking *ACO1* (*aco1*Δ) is included for comparison. (**B**) Wild-type BY4741 and *pif1*Δ cells were grown for 24 h in the absence (white bars) or the presence (black bars) of 5 mM $ZnCl_2$, and aconitase activity was measured. (**C**) Cells were grown as in (**B**) and samples were processed to quantify total (black bars), mitochondrial (white bars) and non-mitochondrial (hatched bars) aconitase protein using an ELISA method (see the Experimental section). In all cases, results are means ± S.D. for four independent experiments. (**D**) Dilutions of the indicated strains (BY4741 background) were spotted on to YPD plates in the presence or the absence of 7 mM $ZnCl_2$. Growth was monitored after 3 days.

that, in the absence of Pif1, Aco1, would shift from having an enzymatic role in the tricarboxylic acid cycle to an mtDNA-binding function. This would be consistent with the incapacity of the *pif1*Δ mutant to grow on respiratory carbon sources [13,34] and would explain, by a feedback mechanism, the increased expression of *ACO1* observed in *pif1*Δ cells. It is suggestive that *IDH1*, which also associates to the mitochondrial nucleoid [35], is also induced in the absence of *PIF1* (Table 2). Further support for our hypothesis comes from our observation that cells expressing the K264A version of Pif1, which lacks helicase activity but still retains the capacity to bind DNA [15], display a zinc-sensitivity phenotype indistinguishable from that of the wild-type strain (Figure 1A) and contain aconitase activity (Figure 8A). Expression of mitochondrially-targeted Pif1 significantly decreases the tolerance to the metal caused by the gene deletion. In contrast, expression in the *pif1*Δ background of a nuclear-targeted version of Pif1 results in a phenotype equivalent to that of the gene deletion (i.e. increased zinc tolerance) and absence of aconitase activity. It is worth noting that cells expressing the mitochondrially targeted Pif1-m2, which display significant, but lower-than-normal levels of aconitase activity, do not completely mimic the sensitivity to zinc of wild-type cells (Figure 1A). Failure to achieve a full wild-type phenotype could be due to a leakage of this protein to the nucleus, as proposed by Schulz and Zakian [16]. All of these evidences demonstrate a relationship between the absence of Pif1 in the mitochondria, the levels of aconitase activity and the tolerance to zinc in yeast cells.

It is more difficult to explain why the mitochondrial lack of Pif1 leads to increased zinc tolerance. One possibility would be that this effect is derived from the absence of aconitase activity (as suggested by Figure 8D). The aconitase system is generally accepted as a major marker of iron-sulfur-cluster status in the cell [36] and, in turn, proper formation of iron-sulfur-cluster proteins represents an important signal for iron homoeostatic mechanisms. It is suggestive that our transcriptomic profiling of *pif1*Δ cells, reveals a 2–3-fold increase in the expression of *ACO1* and *ACO2* genes, as well as of *LEU1* and *LYS4*. *LEU1* and *LYS4* encode aconitase-like proteins which, similarly to Aco1, are iron-sulfur proteins of the [4Fe-4S] type [37,38]. Blocking of iron-sulfur biogenesis results in increased intracellular or mitochondrial iron content, as in the case of mutation of *NFS1* [39], *YTH1* (frataxin) [40] or *GRX5* [41]. In addition, a recent report [42] has highlighted the fact that loss of mtDNA interferes with iron-sulfur cluster biogenesis. We suggest that the mtDNA-related function assumed by Aco1 (and perhaps Idh1) in the absence of Pif1 could lead to a misbalance of iron homoeostasis, causing an accumulation of iron in the mitochondria which, subsequently, would explain the capacity of *pif1*Δ cells to cope with zinc overload. Alternatively, sequestration of zinc in the mitochondria by still unknown mechanisms might be the basis for the zinc tolerance of the *pif1*Δ mutant. The accumulation of iron might be a consequence of increased iron uptake (although we do not observe induction of genes encoding reductive iron transporters), triggered by a possible dissociation of iron-sulfur clusters from Aco1 or other iron-sulfur-cluster-containing proteins. It should be noted that we do not observe induction of *FET3*, which has been reported as a marker of impaired iron-sulfur cluster biosynthesis [19], indicating that this process is not altered in *pif1* mutants. Dissociation of the iron-sulfur cluster may release sulfur, which may explain the inhibition of genes related to sulfur utilization identified in our microarray experiments.

In essence, our experiments define a scenario in which the moonlighting nature of yeast aconitase would be at the crossroad of the pleiotropic effect of *pif1*Δ deletion. Alteration in the mitochondrial aconitase function would trigger a domino effect on iron homoeostasis that might result in the altered zinc tolerance

originally identified in the *pif1*Δ mutant [6], thus constituting a remarkable example of the intimate connection existing between the homoeostatic mechanisms of different metals [43]. Further work is being undertaken to molecularly define the relationships between cellular aconitase functions and metal (zinc and iron) metabolism regulation.

AUTHOR CONTRIBUTION

María Guirola and Lina Barreto performed most of the experiments. Ayelen Pagani and Miriam Romagosa contributed in the early stages of the project to the experimental work. Antonio Casamayor, carried out the microarray experiments and analysed the data. Silvia Atrian and Joaquín Ariño designed the research strategy, supervised and integrated the experiments and wrote the manuscript.

ACKNOWLEDGEMENTS

We thank V.A. Zakian for yeast strains,M. Geli, A. Dancis and D. Pain for antibodies, and D. Winge and D. Eide for fruitful discussions and advice. We also thank R. Rothstein (Department of Genetics and Development, Columbia University, New York, U.S.A.) and D. Botstein (Lewis–Sigler Institute for Integrative Genomics, Princeton University, Princeton, NJ, U.S.A.) for yeast strains. The excellent technical assistance of A. Vilalta and M. Robledo is acknowledged. We also thank the 'Serveis Científico-Tècnics' of the University of Barcelona for metal measurements.

FUNDING

This work was supported by the European Union Systems Biology of Microorganisms programme [grant numbers GEN2006–27748-C2–1-E/SYS, EUI2009–04147 (to J.A.)] and by the Ministerio de Ciencia e Innovacion, Spain [grant numbers BFU2008–04188-C03–01 (to J.A.), BFU2007–60342 and BFU2009–11593 (to A.C.), BIO2009–12513-C02–01 (to S.A.)]. J.A. and S.A. are recipients of 'Ajut de Suport a les Activitats dels Grups de Recerca', Generalitat de Catalunya [grant numbers 2009SGR-1091 (to J.A), 2009SGR-1457 to S.A.]. M.G. is a recipient of a Ministerio de Asuntos Exteriores y de Cooperación-Agencia Española de Cooperación Internacional fellowship.

REFERENCES

1 Eide, D. J. (2009) Homeostatic and adaptive responses to zinc deficiency in *Saccharomyces cerevisiae*. J. Biol. Chem. **284**, 18565–18569
2 Macdiarmid, C. W., Milanick, M. A. and Eide, D. J. (2002) Biochemical properties of vacuolar zinc transport systems of *Saccharomyces cerevisiae*. J. Biol. Chem. **277**, 39187–39194
3 Macdiarmid, C. W., Gaither, L. A. and Eide, D. (2000) Zinc transporters that regulate vacuolar zinc storage in *Saccharomyces cerevisiae*. EMBO J. **19**, 2845–2855
4 Ramsay, L. M. and Gadd, G. M. (1997) Mutants of *Saccharomyces cerevisiae* defective in vacuolar function confirm a role for the vacuole in toxic metal ion detoxification. FEMS Microbiol. Lett. **152**, 293–298
5 Regalla, L. M. and Lyons, T. (2006) Zinc in yeast: mechanisms involved in homeostasis. In Molecular Biology of Metal Homeostasis and Detoxification: From Microbes to Man (Tamás, M. and Martinoia, E., eds), pp. 37–58, Springer-Verlag, Berlin
6 Pagani, M. A., Casamayor, A., Serrano, R., Atrian, S. and Arino, J. (2007) Disruption of iron homeostasis in *Saccharomyces cerevisiae* by high zinc levels: a genome-wide study. Mol. Microbiol. **65**, 521–537
7 Wu, C. Y., Bird, A. J., Winge, D. R. and Eide, D. J. (2007) Regulation of the yeast TSA1 peroxiredoxin by ZAP1 is an adaptive response to the oxidative stress of zinc deficiency. J. Biol. Chem. **282**, 2184–2195
8 Foury, F. and Kolodynski, J. (1983) pif mutation blocks recombination between mitochondrial rho$^+$ and rho$^-$ genomes having tandemly arrayed repeat units in *Saccharomyces cerevisiae*. Proc. Natl. Acad. Sci. U.S.A. **80**, 5345–5349
9 Bochman, M. L., Sabouri, N. and Zakian, V. A. (2010) Unwinding the functions of the Pif1 family helicases. DNA Repair **9**, 237–249
10 Cheng, X., Dunaway, S. and Ivessa, A. S. (2007) The role of Pif1p, a DNA helicase in *Saccharomyces cerevisiae*, in maintaining mitochondrial DNA. Mitochondrion **7**, 211–222
11 Lahaye, A., Stahl, H., Thines-Sempoux, D. and Foury, F. (1991) PIF1: a DNA helicase in yeast mitochondria. EMBO J. **10**, 997–1007
12 Lahaye, A., Leterme, S. and Foury, F. (1993) PIF1 DNA helicase from *Saccharomyces cerevisiae*: biochemical characterization of the enzyme. J. Biol. Chem. **268**, 26155–26161
13 Van Dyck, E., Foury, F., Stillman, B. and Brill, S. J. (1992) A single-stranded DNA binding protein required for mitochondrial DNA replication in *S. cerevisiae* is homologous to *E. coli* SSB. EMBO J. **11**, 3421–3430
14 Zhou, J., Monson, E. K., Teng, S. C., Schulz, V. P. and Zakian, V. A. (2000) Pif1p helicase, a catalytic inhibitor of telomerase in yeast. Science **289**, 771–774
15 Boule, J. B., Vega, L. R. and Zakian, V. A. (2005) The yeast Pif1p helicase removes telomerase from telomeric DNA. Nature **438**, 57–61
16 Schulz, V. P. and Zakian, V. A. (1994) The *Saccharomyces* PIF1 DNA helicase inhibits telomere elongation and de novo telomere formation. Cell **76**, 145–155
17 Chen, X. J., Wang, X., Kaufman, B. A. and Butow, R. A. (2005) Aconitase couples metabolic regulation to mitochondrial DNA maintenance. Science **307**, 714–717
18 Chen, X. J., Wang, X. and Butow, R. A. (2007) Yeast aconitase binds and provides metabolically coupled protection to mitochondrial DNA. Proc. Natl. Acad. Sci. U.S.A. **104**, 13738–13743
19 Chen, O. S., Crisp, R. J., Valachovic, M., Bard, M., Winge, D. R. and Kaplan, J. (2004) Transcription of the yeast iron regulon does not respond directly to iron but rather to iron-sulfur cluster biosynthesis. J. Biol. Chem. **279**, 29513–29518
20 Jeffery, C. J. (2009) Moonlighting proteins: an update. Mol. Biosyst. **5**, 345–350
21 Gancedo, C. and Flores, C. L. (2008) Moonlighting proteins in yeasts. Microbiol. Mol. Biol. Rev. **72**, 197–210
22 Alberola, T. M., Garcia-Martinez, J., Antunez, O., Viladevall, L., Barcelo, A., Arino, J. and Perez-Ortin, J. E. (2004) A new set of DNA macrochips for the yeast *Saccharomyces cerevisiae*: features and uses. Int. Microbiol. **7**, 199–206
23 Viladevall, L., Serrano, R., Ruiz, A., Domenech, G., Giraldo, J., Barcelo, A. and Arino, J. (2004) Characterization of the calcium-mediated response to alkaline stress in *Saccharomyces cerevisiae*. J. Biol. Chem. **279**, 43614–43624
24 Herrero, J., Al Shahrour, F., Diaz-Uriarte, R., Mateos, A., Vaquerizas, J. M., Santoyo, J. and Dopazo, J. (2003) GEPAS: A web-based resource for microarray gene expression data analysis. Nucleic Acids Res. **31**, 3461–3467
25 Brazma, A. and Vilo, J. (2000) Gene expression data analysis. FEBS Lett. **480**, 17–24
26 Hong, E. L., Balakrishnan, R., Dong, Q., Christie, K. R., Park, J., Binkley, G., Costanzo, M. C., Dwight, S. S., Engel, S. R., Fisk, D. G. et al. (2008) Gene ontology annotations at SGD: new data sources and annotation methods. Nucleic Acids Res. **36**, D577–D581
27 Lyons, T. J., Villa, N. Y., Regalla, L. M., Kupchak, B. R., Vagstad, A. and Eide, D. J. (2004) Metalloregulation of yeast membrane steroid receptor homologs. Proc. Natl. Acad. Sci. U.S.A. **101**, 5506–5511
28 Crisp, R. J., Adkins, E. M., Kimmel, E. and Kaplan, J. (2006) Recruitment of Tup1p and Cti6p regulates heme-deficient expression of Aft1p target genes. EMBO J. **25**, 512–521
29 Crisp, R. J., Pollington, A., Galea, C., Jaron, S., Yamaguchi-Iwai, Y. and Kaplan, J. (2003) Inhibition of heme biosynthesis prevents transcription of iron uptake genes in yeast. J. Biol. Chem. **278**, 45499–45506
30 Camadro, J. M. and Labbe, P. (1988) Purification and properties of ferrochelatase from the yeast *Saccharomyces cerevisiae*: evidence for a precursor form of the protein. J. Biol. Chem. **263**, 11675–11682
31 Hao, Q. and Maret, W. (2005) Imbalance between pro-oxidant and pro-antioxidant functions of zinc in disease. J. Alzheimers Dis. **8**, 161–170
32 Kucej, M. and Butow, R. A. (2007) Evolutionary tinkering with mitochondrial nucleoids. Trends Cell Biol. **17**, 586–592
33 Shadel, G. S. (2005) Mitochondrial DNA, aconitase 'wraps' it up. Trends Biochem. Sci. **30**, 294–296
34 O'Rourke, T. W., Doudican, N. A., Mackereth, M. D., Doetsch, P. W. and Shadel, G. S. (2002) Mitochondrial dysfunction due to oxidative mitochondrial DNA damage is reduced through cooperative actions of diverse proteins. Mol. Cell. Biol. **22**, 4086–4093
35 Chen, X. J. and Butow, R. A. (2005) The organization and inheritance of the mitochondrial genome. Nat. Rev. Genet. **6**, 815–825
36 Pierik, A. J., Netz, D. J. and Lill, R. (2009) Analysis of iron-sulfur protein maturation in eukaryotes. Nat. Protoc. **4**, 753–766
37 Lill, R., Dutkiewicz, R., Elsasser, H. P., Hausmann, A., Netz, D. J., Pierik, A. J., Stehling, O., Urzica, E. and Muhlenhoff, U. (2006) Mechanisms of iron-sulfur protein maturation in mitochondria, cytosol and nucleus of eukaryotes. Biochim. Biophys. Acta **1763**, 652–667
38 Lill, R. and Muhlenhoff, U. (2008) Maturation of iron-sulfur proteins in eukaryotes: mechanisms, connected processes, and diseases. Annu. Rev. Biochem. **77**, 669–700
39 Li, J., Kogan, M., Knight, S. A., Pain, D. and Dancis, A. (1999) Yeast mitochondrial protein, Nfs1p, coordinately regulates iron-sulfur cluster proteins, cellular iron uptake, and iron distribution. J. Biol. Chem. **274**, 33025–33034

40 Santos, R., Dancis, A., Eide, D., Camadro, J. M. and Lesuisse, E. (2003) Zinc suppresses the iron-accumulation phenotype of *Saccharomyces cerevisiae* lacking the yeast frataxin homologue (Yfh1). Biochem. J. **375**, 247–254
41 Rodriguez-Manzaneque, M. T., Tamarit, J., Belli, G., Ros, J. and Herrero, E. (2002) Grx5 is a mitochondrial glutaredoxin required for the activity of iron/sulfur enzymes. Mol. Biol. Cell **13**, 1109–1121
42 Veatch, J. R., McMurray, M. A., Nelson, Z. W. and Gottschling, D. E. (2009) Mitochondrial dysfunction leads to nuclear genome instability via an iron-sulfur cluster defect. Cell **137**, 1247–1258

Received 13 July 2010/9 September 2010; accepted 21 September 2010
Published as BJ Immediate Publication 21 September 2010, doi:10.1042/BJ20101032

43 Atkinson, A. and Winge, D. R. (2009) Metal acquisition and availability in the mitochondria. Chem. Rev. **109**, 4708–4721
44 Sikorski, R. S. and Hieter, P. (1989) A system of shuttle vectors and yeast host strains designed for efficient manipulation of DNA in *Saccharomyces cerevisiae*. Genetics **122**, 19–27
45 Eisen, M. B., Spellman, P. T., Brown, P. O. and Botstein, D. (1998) Cluster analysis and display of genome-wide expression patterns. Proc. Natl. Acad. Sci. U.S.A. **95**, 14863–14868

Biochem. J. (2010) **432**, 595–605 (Printed in Great Britain) doi:10.1042/BJ20101032

online data

SUPPLEMENTARY ONLINE DATA

Lack of DNA helicase Pif1 disrupts zinc and iron homoeostasis in yeast

María GUIROLA*[1], Lina BARRETO†[1], Ayelen PAGANI*, Miriam ROMAGOSA*, Antonio CASAMAYOR†, Silvia ATRIAN*[2] and Joaquín ARIÑO†[2,3]

*Departament de Genètica and Institut de Biomedicina, Universitat de Barcelona, Barcelona, Spain, and †Departament de Bioquímica i Biologia Molecular and Institut de Biotecnologia i Biomedicina, Universitat Autònoma de Barcelona, Bellaterra 08193, Barcelona, Spain

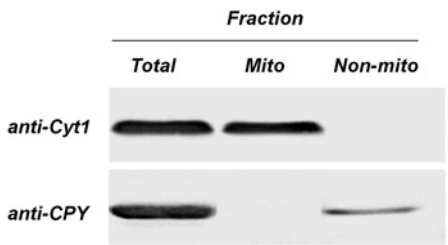

Figure S1 Purified mitochondrial fractions

Mitochondrial fractions were purified with the MitoISO3 kit (Sigma–Aldrich) as described in the main text. A total of 30 mg of total extracts, mitochondrial fractions (Mito) and the last supernatant (Non-mito) were resolved by PAGE (12.5% gels) and transferred on to Hybond–PVDF membranes. Membranes were incubated with anti-Cyt1 (mitochondrial marker) or anti-carboxypeptidase Y (CPY, vacuolar marker) antibodies. The anti-(rabbit IgG)–horseradish peroxidase antibody (from donkey, dilution 1:10000) was used as a secondary antibody and signals were developed with enhanced chemiluminescence.

[1] These authors contributed equally to this work.
[2] These authors contributed equally as co-last authors.
[3] To whom correspondence should be addressed (email joaquin.arino@uab.es).

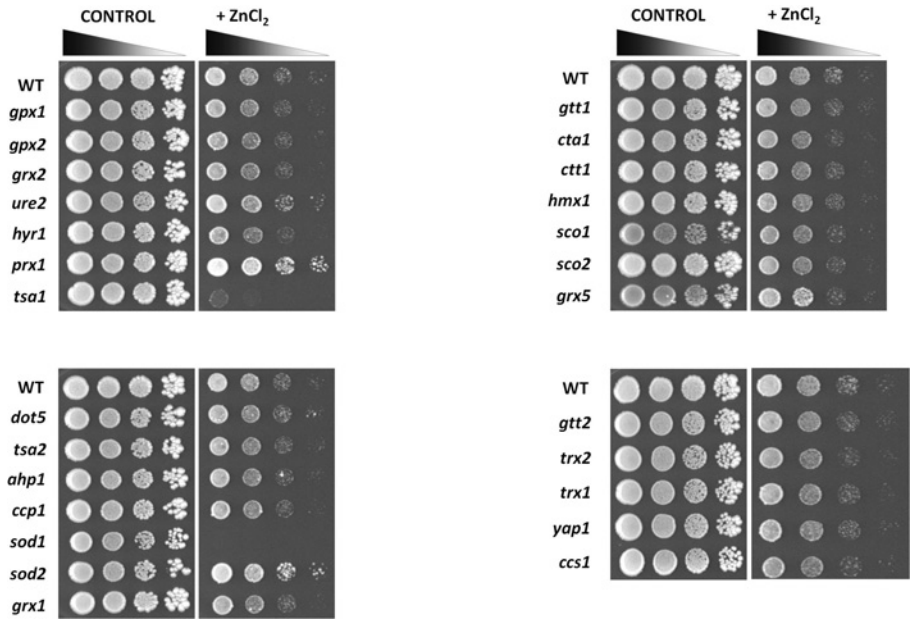

Figure S2 Zinc tolerance of *kanMX*-deletion derivative strains

Dilutions (1:10) of wild-type strain BY4741 and the indicated *kanMX*-deletion derivatives were spotted on to YPD plates containing 5 mM $ZnCl_2$ and grown for 4 days.

Received 13 July 2010/9 September 2010; accepted 21 September 2010
Published as BJ Immediate Publication 21 September 2010, doi:10.1042/BJ20101032